Techno-Economic Potential Evaluation of Small-Scale off-Grid Renewable Power Systems in Xinjiang, China*

PU Xiaohua, GU Wenbo†

(*School of Electrical Engineering, Xinjiang University, Urumqi Xinjiang 830017, China*)

Abstract: A hybrid energy system is built for the power demand of a community in Xinjiang of China, and pumped storage and lithium batteries are used as energy storage devices. The feasibility of different configurations is evaluated through techno-economic analysis. Technical-economic parameters are set in the HOMER Pro software to obtain optimal configuration and techno-economic evaluation and sensitivity analysis. The study also explores the impact of different types of PV tracking systems and module costs on system performance. The results show that the lowest levelized cost of energy (LCOE) (0.135 $/kWh) can be achieved with pumped hydro, which is more economical than lithium batteries. PV tracking systems can improve solar efficiency. Compared with diesel systems, renewable energy has economic advantages and environmental benefits. In most regions of Xinjiang, solar energy is more competitive than wind power. In areas with abundant wind resources, the integration of wind and solar energy can reduce costs.

Key words: net present cost; levelized cost of energy; renewable energy system; capacity sizing

DOI: 10.13568/j.cnki.651094.651316.2024.12.05.0002

CLC number: TM615 **Document Code**: A **Article ID**: 2096-7675(2025)02-0168-018

引文格式: 蒲晓华, 顾文波. 中国新疆地区小型离网可再生能源发电系统的技术经济潜力评价[J]. 新疆大学学报(自然科学版中英文), 2025, 42(2): 168-185.

英文引文格式: PU Xiaohua, GU Wenbo. Techno-economic potential evaluation of small-scale off-grid renewable power systems in Xinjiang, China[J]. Journal of Xinjiang University(Natural Science Edition in Chinese and English), 2025, 42(2): 168-185.

中国新疆地区小型离网可再生能源发电系统的技术经济潜力评价

蒲晓华, 顾文波

(新疆大学 电气工程学院, 新疆 乌鲁木齐 830017)

摘 要: 针对中国新疆某社区的电力需求搭建离网风光储能系统, 以抽水蓄能和锂电池作为储能设备. 通过技术经济分析评估不同配置方案的可行性. 在HOMER Pro软件中设定技术经济参数. 对系统进行容量优化、技术经济评估及敏感性分析. 还探讨不同类型光伏跟踪系统以及组件成本对技术经济性的影响. 结果表明: 搭配抽水蓄能可以达到最低的平准化度电成本（LCOE）(0.135 $/kWh), 相比锂电池更经济. 光伏跟踪系统可提高光伏的发电效率. 与纯柴油系统相比, 新能源具有明显的成本优势和环境效益. 新疆大部分地区太阳能比风能更具竞争力, 而在风力资源丰富地区, 风光能源的集成可以进一步降低能源成本.

关键词: 净现值; 平准化度电成本; 可再生能源系统; 容量配置

* **Received Date:** 2024-12-05

Foundation Item: This work was supported by Natural Science Foundation of Xinjiang Uygur Autonomous Region of China "Research on photoelectric thermal conversion mechanism and optimization design of photovoltaic building envelope structure" (2022D01C87).

Biography: PU Xiaohua (1999—), male, master student, research field: renewable energy system, E-mail: 107552201485@stu.xju.edu.cn.

† **Corresponding author:** GU Wenbo (1992—), male, associate professor, research field: solar system and integrated electrothermal management, E-mail: bobo1314@sjtu.edu.cn.

0 Introduction

The future energy framework necessitates broad participation from renewable sources to address human development and common interests[1]. To achieve the Paris Agreement's goal of limiting global temperature rise below 2 ℃, China has set carbon peaking and neutrality goals, promoting green energy transitions nationwide[2−4]. Establishing its carbon market and investing in renewable energy industries underscores China's commitment to energy security and sustainability[4−6]. Northwest China stands out as pivotal for renewable energy research and industrialization due to favorable conditions that facilitate large-scale power plant construction, laying a strong foundation for renewable energy utilization[7−9]. The utilization scale of photovoltaic (PV) and wind turbines (WT) increases year by year. However, structural challenges within the renewable sector cannot be ignored. Renewable energy's inherent volatility and uncertainty contribute to frequent energy shortages or excesses, posing significant risks to energy systems and grids[10−12]. Hybrid energy systems incorporating sufficient storage facilities offer a viable solution, balancing supply and demand through complementary equipment configurations[13−15]. Accelerating technological development in remote areas, exemplified by wind farms and solar stations, faces transmission capacity limitations and high grid expansion costs, prompting interest in off-grid systems for their economic benefits and self-sufficiency potential[16−19]. Research on off-grid hybrid systems has utilized mathematical methodologies, heuristic algorithms, reinforcement learning, and commercial modeling software like HOMER, SAM, and PVsyst[20−23].

Various case studies highlight the efficacy of hybrid systems across various settings. For instance, a non-residential consumer in Iran benefited from a PV/WT/Battery system with an LCOE of 9.3∼12.6 ¢/kWh[24]. Consumers in Egypt can get LCOE of 2.1 ¢/kWh with a grid-connected PV/WT system, which is lower than the retail electricity price (6.9 ¢/kWh)[25]. In Malawi, grid-connected PV/Biogas system can achieve optimal LCOE at 0.095 $/kWh[26]. Similar initiatives in Baluchistan can have lower pollution gas emission (64%) and LCOE (0.3 $/kWh) than diesel generators (DG) system[27]. In Malaysia, optimized systems can obtain LCOE of 0.279 $/kWh with 41.6% renewable fraction (RF)[28]. Investigations in India revealed advantages of PV/WT/DG/Battery configurations across different cities[29]. Further, particle swarm optimization (PSO) was used in Algerian villages for energy system design, showing the minimum LCOE of 0.37 $/kWh under 93% renewable fraction[30]. Seawater desalination projects in Jordan demonstrated PV/WT/DG/Batteries system has LCOE of 0.063 $/kWh and RF of 98.2% and reduction of CO_2[31]. Strategies like combined dispatch (CD) and load following (LF) were evaluated for their impacts on emissions and LCOE[32], and the evaluation of LCOE is similar for different dispatch strategies (0.31∼0.33 $/kWh) for both PV/DG/LA and PV/DG/Li-ion and RF is significantly higher (77%∼80%) in LF than the CD (59%∼62%) and the CC (32%∼52%) strategies. PV/DG systems could meet all loads at minimal costs in different scenarios[33]. Cases of hybrid energy systems were studied to supply electricity demand. The optimum configuration could obtain minimum LCOE of 5.12 INR/kWh in a grid-connected system and 16.12 INR/kWh in an off-grid system for the electrical load of a residential house in India[34]. PV-based systems on Yongxing Island can reduce LCOE and CO_2 by 3.7% and 4.3%[35]. Hydrogen storage has economic benefits for long-term energy storage which can reduce costs to the lowest LCOE (0.50 $/kWh) in Colorado[36]. Sensitivity analyses highlighted the importance of capital costs and discount rates in determining LCOE and renewable fractions[37]. PV/Wind/Hydro/Pumpedhydrostorage (PHS) can have lower LCOE (0.136 $/kWh) compared to the DG system (0.355 $/kWh) in Canada[38]. A hybrid WT/DG/Battery system for 280 homes in Lanzhou can obtain the optimal net present cost (NPC) of $7.73 M and LCOE of 0.471 $/kWh[39]. In different PV tracking methods, the dual-axis tracker achieved maximum power, highest PV penetration, and lowest LCOE and NPC. Sensitivity analysis showed that temperature, wind speed, and hub height are key factors for PV/WT systems[40].

The review of the previous research works indicates that renewable energy systems consisting of different components have been investigated to satisfy the electric supply, and the overall techno-economic performance analysis has been carried out. Researchers have explored different regions, system compositions, and strategies, and analyzed indicators such as LCOE, NPV, LPSP, and excess electricity under different scenarios. However, the detailed and comprehensive analysis of various configurations of hybrid power systems in the Northwest zones of China is still inadequate in previous studies, potentially limiting the selection of optimal systems and future development. Furthermore, few studies have thoroughly evaluated the practical performance of different PV tracking systems within hybrid energy systems or considered the dynamic effects of market adjustments and industry improvements on system costs. The dynamics of market adjustment and the industry improvement may fluctuate costs, misleading practical decisions adversely.

To address these limitations, this paper aims to explore the application potential of PV/WT/PHS-based energy systems in cold climate regions of Northwest China. Several cities in Xinjiang Uygur Autonomous Region of China are selected to deploy the energy systems. By modeling renewable energy systems with diverse electricity generation and storage components, we conduct a comprehensive evaluation of the potential and performance of different hybrid power system configurations. Additionally, an analysis of different photovoltaic tracking systems is also conducted to examine the practical impact on the overall renewable energy system. Sensitivity analysis is also carried out to describe the effects of variables such as price of components and technical parameters. Our research provides insights into the optimal hybrid power system configuration for cold climates, supporting decision-making for future renewable energy projects and policies in Northwest China.

1 System Description

HOMER Pro optimization tool is employed to optimize various models and evaluate the suitability of hybrid systems with solar PV panels, WT and PHS for a residential community in Urumqi. The project was compared with an alternative configuration utilizing Lithium-ion (Li^+) battery bank to meet an equivalent load demand. Furthermore, the economic and environmental advantages of these hybrid systems are investigated in contrast to a conventional diesel-only power source.

1.1 Modelling and Initial System Design

This study involves several system components with different functions. The energy generation configuration includes PV, WT and DG, and the energy storage options include PHS and battery bank, as shown in Fig 1. Converters are also essential for electricity conversion throughout the system. HOMER Pro necessitates several input parameters, including project lifetime, hourly resource data and load data, architecture metrics, detailed technical and economic specifications of components[41]. The lifespan of the project has been established as a twenty-year duration. The nominal discount rate is adopted as 8%, reflecting a cautious approach for renewable energy initiatives, while the inflation rate is estimated at 2%. The penalty for anticipated capacity shortage has been set at zero.

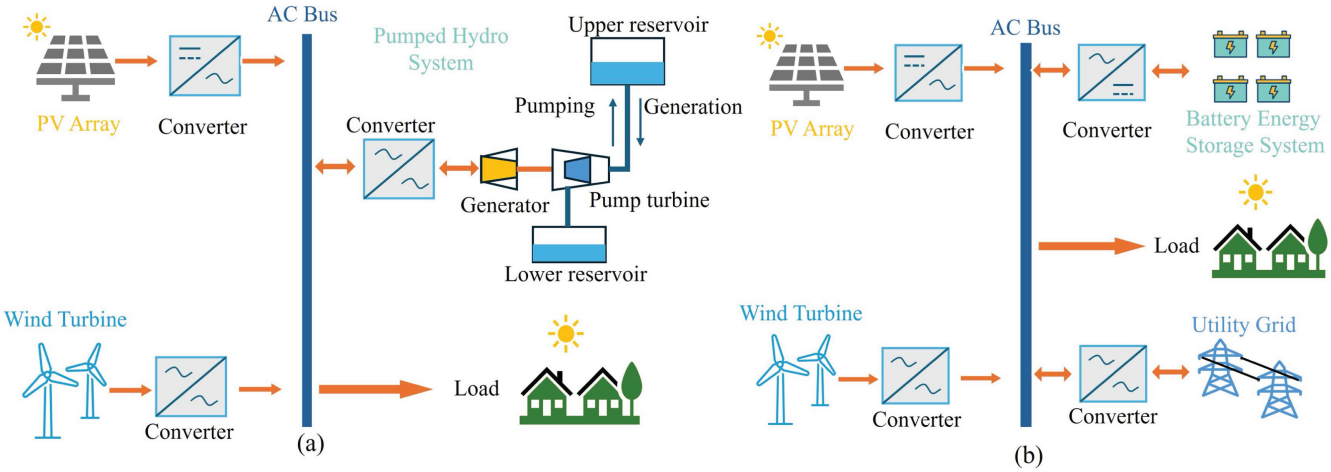

Fig 1 Configurations of off-grid systems (a)PV/WT/PHS, (b) PV/WT/Battery

1.2 Load Profile

The proposed system would serve a community consisting of 210 family households, 3 shops, 1 school, 1 clinic and 1 community office, located in Xinjiang Uygur Autonomous Region of China. As shown in Fig 2, the daily average electricity consumption of this community is set at 2 024.8 kWh. The load demands may be affected by synthesis factors, such as weather conditions, economic criteria, and geographic location. Therefore, based on the comprehensive conditions, the daily and hourly randomness is set as 12% and 8% to make the calculation result more convincing and practical. The average hourly power for users is 84 kW, while the peak power can reach 245 kW throughout the year. The peak user load throughout the year is concentrated from May to September. The peak load of the day is mainly between 18 and 22 o'clock in the afternoon.

1.3 Resources Assessment

Xinjiang exhibits a typical temperate continental climate characterized by its arid conditions, with an average annual precipitation of approximately 297 mm[42–43]. In accordance with building energy consumption thermal management standards, this locale qualifies as a cold climate zone, with nighttime temperatures averaging 4 ℃ and daytime temperatures averaging 13 ℃ annually[44]. The region possesses significant natural resources, particularly in wind and solar energy, rendering it well-suited for practical applications of renewable energy sources.

In accordance with the mean data downloaded from the NASA Surface Meteorology and Solar Energy website[45], the hourly data for solar irradiation, wind speed, and ambient temperature in Urumqi are presented in Fig 3.

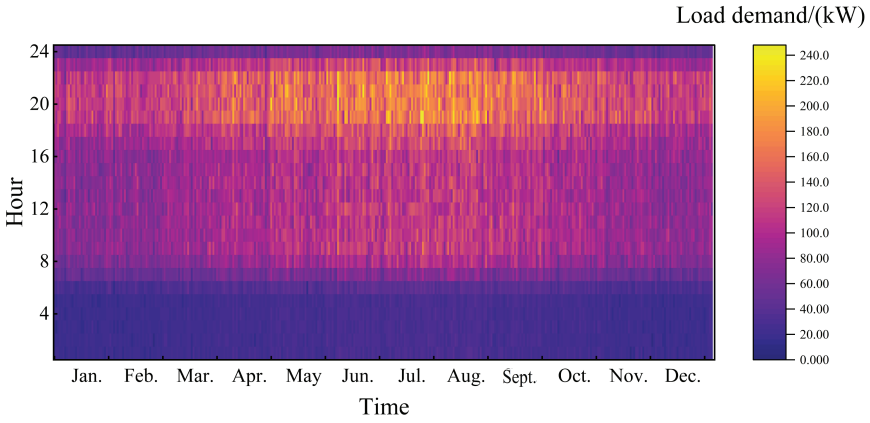

Fig 2 Load profile of proposed community

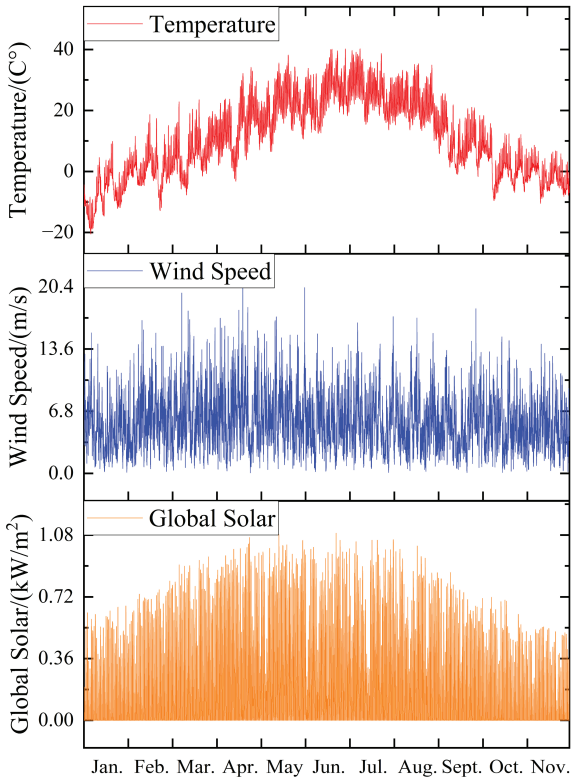

Fig 3 Hourly data for solar irradiation, wind speed, and ambient temperature in Urumqi

The monthly solar irradiation data is displayed in Fig 4. Notably, the solar irradiation levels exhibit a seasonal pattern, with higher values observed during the summer months (May to July) and lower values during the winter months (November to January of next year). The average monthly solar irradiation reaches its peak at 0.275 kW/m^2 in May and reaches its lowest point at 0.097 kW/m^2 in December.

The wind speed within the region exhibits significant variations, ranging from 0 to 20 m/s at a height of 50 meters. The average annual wind speed is recorded at 4.26 m/s, as depicted in Fig 4 and Fig 5. This favorable wind condition enables the region to harness clean and emission-free wind energy.

2 Modelling, Simulation and Optimization

2.1 Components

2.1.1 Solar PV

This study examined PV solar module with a rated capacity of 1 kW and a panel efficiency of 20.40%. The derating factor for the photovoltaic panel is established at 90%, while the power temperature coefficient is set at -0.41%/℃. The power output generation of PV modules can be calculated using the following equation[40]:

$$P_{\mathrm{PV}} = Y_{\mathrm{PV}} f_{\mathrm{PV}} \left(\frac{G}{G_{\mathrm{STC}}}\right)[1+\alpha_p(T_c - T_{c,\mathrm{STC}})], \tag{1}$$

where Y_{PV} is the rated capacity of PV array (kW); f_{PV} is the derating factor (90%); G is the incident solar irradiation on the PV array (kW/m^2) at each time step; G_{STC} is the incident solar irradiation at standard test conditions (1 kW/m^2); α_p is the temperature coefficient of power (-0.41%/℃); T_c is the PV cell temperature (℃); and $T_{c,\mathrm{STC}}$ is the PV cell temperature under standard test conditions (25 ℃).

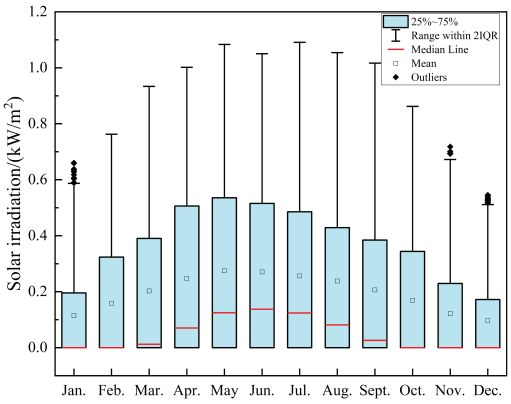

Fig 4 Solar irradiation in Urumqi

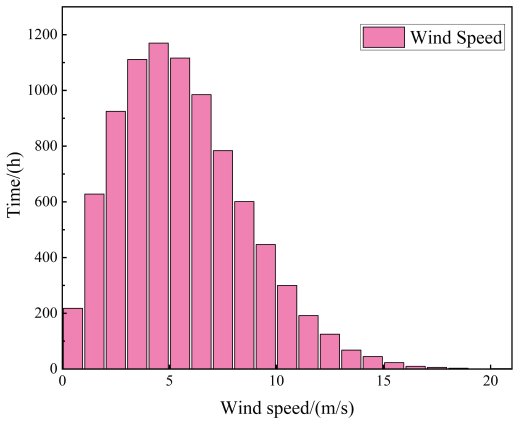

Fig 5 Wind speed status of Urumqi

The cell temperature T_c can be obtained from the energy balance of the PV module[46]:

$$\tau\alpha G_t = \eta_{\mathrm{PV}} G + U_{\mathrm{L}}(T_c - T_a), \tag{2}$$

where $\tau\alpha$ is the effective transmittance-absorptance of PV array; η_{PV} is the PV panel efficiency (20.4%), U_{L} is the heat transfer coefficient (kW/(m^2·℃)); T_a is the ambient temperature (℃). Equation (2) can be rewritten as follows:

$$T_c = T_a + G\left(\frac{\tau\alpha}{U_{\mathrm{L}}}\right)\left(1 - \frac{\eta_{\mathrm{PV}}}{\tau\alpha}\right). \tag{3}$$

However, the value of $(\tau\alpha/U_{\mathrm{L}})$ is challenging to be measured. Therefore, based on the manufacturer report on the Nominal Operating Cell Temperature (NOCT) which results at 800 W/m^2 solar irradiation, at 20 ℃ ambient temperature, and at no load condition (i.e., η_{PV}=0), the Equation (3) can be rewritten as follows:

$$\frac{\tau\alpha}{U_{\mathrm{L}}} = \frac{T_{c,\mathrm{NOCT}} - T_{a,\mathrm{NOCT}}}{G_{\mathrm{NOCT}}}. \tag{4}$$

It is possible to obtain the final PV cell temperature by using the Equation (5):

$$T_c = T_a + G\frac{T_{c,\mathrm{NOCT}} - T_{a,\mathrm{NOCT}}}{G_{\mathrm{NOCT}}}\left(1 - \frac{\eta_{\mathrm{PV}}}{0.9}\right), \tag{5}$$

whereby HOMER assumes the value of $\tau\alpha$ as 0.9.

The PV module incurs a capital expenditure of 716 $/kW, a replacement cost equivalent to capital cost, and an annual operational cost of 7.2 $/kW[47]. The expected lifespan of the module is 25 years. Parameters of PV are listed in Table 1.

Table 1 Parameters of PV

Parameter	Unit	Specification
Model	-	Generic flat plate PV
Electrical output type	-	Direct current
Rated capacity	kW	1
Derating factor	%	90
Lifetime	years	25
Temperature effect on power	%/°C	-0.41
Efficiency	%	17.3
Dedicated converter efficiency	%	98
Capital cost	$/kW	716
Replacement cost	$/kW	716
Operation and maintenance	$/kW/year	7.2

The selected PV model in base case has no tracking system. To analyze the performance of PV system with PV tracking, different tracking systems are introduced in this paper. PV tracking systems are usually classified into two types, which are single-axis and dual-axis tracking. Three different types of PV models, which are horizontal-axis, vertical-axis and dual-axis, are built in HOMER Pro software. The horizontal-axis tracking system can be seamlessly integrated with various adjustment strategies tailored to specific time intervals, including monthly, weekly, daily, and continuous adjustments. Notably, the vertical-axis and dual-axis systems also offer the option of continuous adjustment[40].

2.1.2 Wind Turbine

In this study, the wind turbine with a rated capacity of 10 kW was selected to adapt to the capacity scale. The power output generation of WT can be calculated by[46]:

$$P_{\mathrm{WT}}=\begin{cases}0, & v\le v_{\mathrm{in}},\\ P_{\mathrm{rated}}\frac{v^3-v_{\mathrm{in}}^3}{v_{\mathrm{out}}^3-v_{\mathrm{in}}^3}, & v_{\mathrm{in}}<v\le v_{\mathrm{rated}},\\ P_{\mathrm{rated}}, & v_{\mathrm{rated}}<v\le v_{\mathrm{out}},\\ 0, & v_{\mathrm{out}}<v,\end{cases} \tag{6}$$

where P_{WT} is the output power of wind turbine (kW); P_{rated} is the rated output power (20 kW); v_{in}, v_{rated} and v_{out} are respectively the cut-in, rated and cut-out characteristic speeds (m/s); and v is the actual wind speed (m/s). The turbine's rated wind speed is set at 15 m/s, while the cut-in speed and cut-out speed are specified as 3 m/s and 25 m/s, respectively. Additionally, the estimated lifetime of the wind turbine is 20 years.

Table 2 Parameters of WT

Parameter	Unit	Specification
Model	-	XANT M-21-ETR
Electrical output type	-	Direct
Number of blades	-	3
Regulation method	-	-
Rated capacity	kW	10
Hub height	m	31.8
Lifetime	years	25
Cut-in wind speed	m/s	3
Cut-out wind speed	m/s	25
Rated wind speed	m/s	15
Capital cost	$/kW	900
Replacement cost	$/kW	900
Operation and maintenance	$/kW/year	9

Table 2 provides the technical specifications of the XANT M-21-ETR model. The chosen WT, which produces AC voltage, possesses a rotor diameter of 20.7 m and a hub height of 31.8 m. The estimated costs for the capital investment,

replacement, as well as operation and maintenance (O&M) of the WT are set at 900 $/kW, 900 $/kW and 9 $/year (1% of the capital cost), respectively[47].

2.1.3 Diesel Generator

DG is a typical choice to generate electricity to supply the off-grid load demand which combusts diesel fuel and releases carbon dioxide (CO_2) and some polluting gases such as carbon monoxide (CO) and nitrogen oxides (NO_x), etc. In this study, the diesel-based systems are considered for the comparison with renewable power, focusing on economic and environmental performance. The fuel consumption of DG in (L/h) is related to the rated powerand output power of DG, which can be described as follows[39]:

$$f_{\mathrm{dg}} = aP_{\mathrm{dgrated}} + bP_{\mathrm{dgout}}, \tag{7}$$

where f_{dg} is the fuel consumption of DG (L/h); P_{dgrated} is the rated power of the DG (270 kW); P_{dgout} is the output power of the DG (kW); a is the fuel curve intercept coefficient (L/kWh); b is the fuel curve slope (L/kWh).

Table 3 outlines the basic specifications of the diesel generator and fuel[39]. The diesel generator is designed with a minimum starting threshold of 25% to ensure a prolonged operational lifespan. The capital cost, replacement cost, and O&M cost are estimated at 370 $/kW, 296 $/kW, and 0.05 $/h[30].

Table 3 Parameters of DG

Parameter	Unit	Specification
Model	-	Auto size genset
Fuel	-	Diesel
Lower heating value	MJ/kg	43.2
Fuel density	kg/m^3	820
Carbon content of fuel	%	88
Sulfur content of fuel	%	0.4
Fuel curve intercept	L/kWh	4.52
Fuel curve slope	L/kWh	0.236
Carbon monoxide (CO) emission	g/L	16.5
Unburned hydrocarbons emission	g/L	0.72
Particulates matter emission	g/L	0.1
Nitrogen oxides (NO_x)	g/L	15.5
Fuel sulfur to PM	%	2.2
Minimum load ratio	%	25
Fuel price	$/L	1
Capital cost	$/kW	370
Replacement cost	$/kW	296
Operation and maintenance	$/h	0.05

2.1.4 Energy Storage System

Energy storage systems can contribute to off-grid systems in achieving energy balance requirements at different time intervals. In the base case, a PHS system has been considered as a viable storage option. It features a 22 kW generator set with an efficiency rating of 90% and a total water reservoir capacity of 1 000 m^3. The nominal voltage is 240 V and the maximum current of charge and discharge is 91.6 A. The capital cost for this PHS system is 1 000 $/kW, while the operational and maintenance costs amount to 100 $/kW/year. Furthermore, the projected lifespan of the PHS system is estimated to be 30 years[38]. The detailed parameters of PHS are presented in Table 4. A PHS builds potential energy by storing water in a reservoir at a certain height when there is excess energy. It converts the potential energy to electricity by releasing the potential energy to turn the turbine generator when there is a demand. The reservoir is located at a certain height above the turbine generator (the head height) to generate potential energy. The flow rate is the amount of water (meters cubed per second) that flows in or out. The following equation is used to calculate the energy storage capacity of a pumped hydro system[48]:

$$E = \frac{9.81\eta\rho V_{\mathrm{res}} H_{\mathrm{head}}}{3.6\times 10^6}, \tag{8}$$

where E is the energy stored (kWh); ρ is the density of water (1 000 kg/m^3); V_{res} is the volume of the reservoir (m^3); H_{head} is the head height (m); η is the efficiency of energy conversion referring to the turbine losses (90%).

As a comparative selection, lithium-ion battery is selected as an available energy storage device to replace pumped storage. The generic 1 kWh Li-ion battery from ASM is employed in this study. The battery energy storage variation is featured by the state of charge (SOC), as shown below[49]:

$$\mathrm{SOC}(i+1)=\mathrm{SOC}(i)+\frac{\eta_{ch}P_{ch}(i)-P_{dis}(i)/\eta_{dis}}{C_{bat}},\ i=1,2,\cdots,8\ 760, \tag{9}$$

where SOC is the state of charge of the batteries (%); i is the time step of the simulation iteration (h); η_{ch} and η_{dis} are the battery charging/discharging efficiency (%); P_{ch} and P_{dis} are the battery charging/discharging power (kW); C_{bat} is the usable capacity of the battery bank (kWh).

Table 4 Parameters of PHS

Parameter	Unit	Specification
Model	-	Generic 245 kWh pumped hydro
Nominal voltage	V	240
Maximum charge current	A	91.6
Maximum discharge current	A	91.6
Generator efficiency	%	90
Head height	m	100
Rated power	kW	20.44
Capacity	kWh	245
Lifetime	years	30
Capital cost	$/kW	1 000
Replacement cost	$/kW	1 000
Operation and maintenance	$/kW/year	200

It is acknowledged that the battery could not be charged and discharged at the same time, the duration of battery charging and discharging are limited as follows[50]:

$$t_{ch}(i)+t_{dis}(i)\le t_{step}, \tag{10}$$

where t_{ch} is the battery charging duration (h), assumed as 1 or 0 in this study; t_{dis} is the battery discharging duration (h), assumed as 1 or 0 in this study; and t_{step} is the time step of the simulation (h), assumed as 1 hour in this study.

To prevent the over-charging and over-discharging for a longer lifetime, some constraints are made for the upper and lower limits of SOC and power of charging and discharging:

$$\mathrm{SOC}_{min}\le\mathrm{SOC}(i)\le\mathrm{SOC}_{max}, \tag{11}$$

$$P_{ch,min}\le P_{ch}(i)\le P_{ch,max}, \tag{12}$$

$$P_{dis,min}\le P_{dis}(i)\le P_{dis,max}, \tag{13}$$

where SOC_{min} and SOC_{max} are the lower and upper limits of SOC (%); $P_{ch,min}$ and $P_{ch,max}$ are the lower and upper limits of power of charging (kW); and $P_{dis,min}$ and $P_{dis,max}$ are the lower and upper limits of power of discharging (kW).

As shown in Table 5, the nominal voltage and nominal capacity are 3.7 V and 1.02 kWh, respectively. The battery system possesses a maximum charge current of 167 A and a maximum discharge current of 500 A. The capital cost, replacement cost, and operation and maintenance cost are estimated at 300 $/kW, 270 $/kW and 3 $/kW/year. It owns a lifetime of 10 years, and can cycle 3 000 times totally[39].

2.1.5 Converter

A bi-directional converter should be implemented to maintain equilibrium in the energy exchange between the DC and AC domains. Energy conversion equipment has different functions: inverters convert DC to AC while rectifiers convert AC to DC. The energy conversion can be calculated as follows[26]:

$$E_{out}=\eta_c E_{in}, \tag{14}$$

where E_{out} is the output energy of converter (kWh); η_c is the efficiency of energy conversion (95%); and E_{in} is the input energy of converter (kWh).

The inverter demonstrates an efficiency of 95%, with a lifespan of 16 years. The rectifier, meanwhile, features a capacity of 100% and an efficiency of 95%. The initial capital costs, replacement costs, and O&M costs for the converter under investigation are assumed to be 300 $/kW, 300 $/kW and 3 $/kW/year, respectively[35]. Table 6 comprehensively summarizes the salient features of the converter.

Table 5 Parameters of Li-ion battery

Parameter	Unit	Specification
Model	-	Generic 1 kWh Li-ion [ASM]
Nominal voltage	V	3.7
Nominal capacity	kWh	1.02
Maximum capacity	Ah	276
Maximum charge current	A	167
Maximum discharge current	A	500
Rate constant	1/h	1
Effective series resistance	ohms	0.000 36
Round-trip efficiency	%	90
Other round-trip losses	%	10
Fixed bulk temperature	°C	20
Lifetime	years	10
Cycle times	-	3 000
Capital cost	$/kW	300
Replacement cost	$/kW	270
Operation and maintenance	$/kW/year	3

Table 6 Parameters of converter

Parameter	Unit	Specification
Model	-	C1-mini-1 000 N
Manufacture	-	Cybo-energy
Inverter efficiency	%	95
Rectifier efficiency	%	95
Relative capacity	%	100
Lifetime	years	16
Capital cost	$/kW	300
Replacement cost	$/kW	300
Operation and maintenance	$/kW/year	3

2.2 System Simulation and Index for Optimization

2.2.1 Description of System Simulation and Optimization

This study develops an integrated model of PV modules, wind turbines, batteries and converters, configured based on system-specific parameters. Meteorological data, system details, and equipment specifications are input for simulations. After modelling and data importing, the simulations will commence by using built-in solver, and the detailed hourly simulations will be performed over a predefined period. Power generation, energy storage charging and discharging, and other relevant metrics are calculated based on the model and input data. The CD strategy is chosen by this study to provide a comprehensive approach to managing renewable energy systems efficiently by integrating multiple resources and optimizing their operation based on real-time demand. The process considers the characteristics and capabilities of each resource to ensure their combined output meets the system's demand. The optimal operating schedule is determined for each resource based on allocated load, considering factors such as resource efficiency, generation costs and constraints. The goal is to find the most economic and reliable dispatch schedule to meet load requirements. Fig 6 illustrates the simulation workflow of HOMER.

2.2.2 Index for Optimization

Loss of power supply probability (LPSP) is a parameter characterizing the stability of the energy supply of the renewable energy system (%). The equations of LPSP can be presented by[51]

$$\mathrm{LPSP}=\frac{E_{\mathrm{unmet}}}{E_{\mathrm{load}}}, \tag{15}$$

where E_{load} is the total annual energy load (kWh); and E_{unmet} is the annual unmet energy load (kWh).

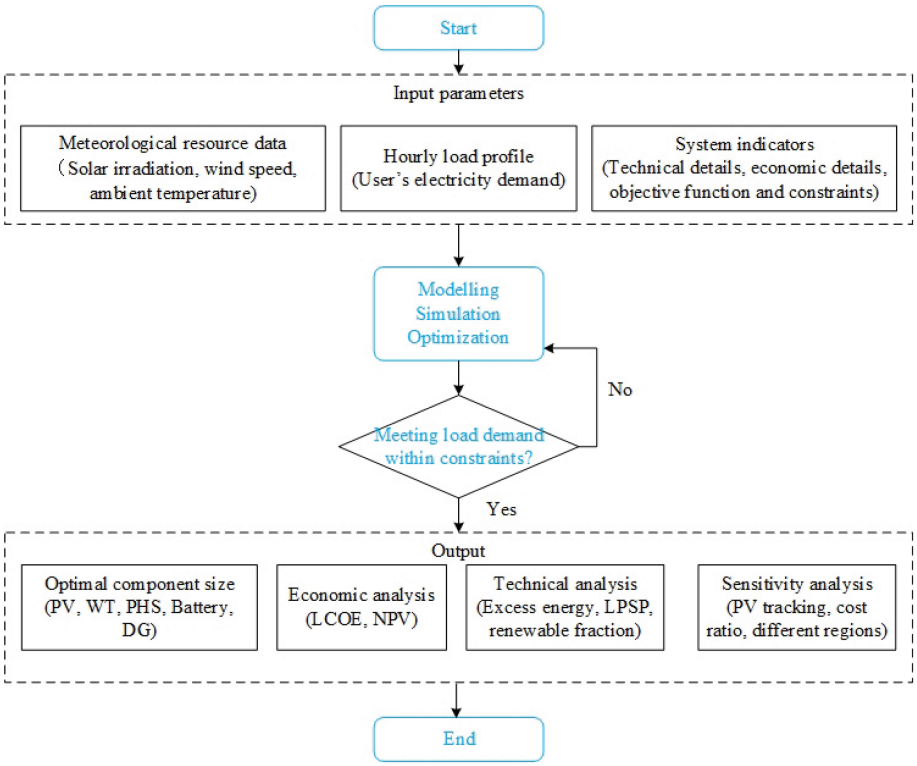

Fig 6 Working framework for optimization using HOMER

The excess energy E_{ex} reflects the amount of energy that cannot be consumed. The equations of excess energy can be presented by[35]

$$E_{\mathrm{ex}}=E_{\mathrm{total}}-E_{\mathrm{s}}, \tag{16}$$

where E_{total} is the total annual generated energy (kWh); and E_s is the total electrical load supplied which is equal to the sum of primary load and deferrable load (kWh).

The net present cost (NPC) refers to the present value encompassing all installation and operational expenses of all components incurred throughout the project's lifespan, while deducting the present value of generated revenues. A financial method for estimating NPC is presented as the following function[52]:

$$C_{\mathrm{A}}=C_{\mathrm{an\_cap}}+C_{\mathrm{O\&M}}+C_{\mathrm{rep}}, \tag{17}$$

$$\mathrm{NPC}=\frac{C_{\mathrm{A}}}{\mathrm{CRF}(d,n)}, \tag{18}$$

$$\mathrm{CRF}(d,n)=\frac{d(d+1)^n}{(d+1)^n-1}, \tag{19}$$

$$d=\frac{d'-f}{1+f}, \tag{20}$$

where C_{A} is the total annualized cost, which is the sum of annual costs of each component (\$); $C_{\mathrm{an\_cap}}$ is the annualized capital cost of a system component (\$); $C_{\mathrm{O\&M}}$ is the operation and maintenance cost (\$); C_{rep} is the replacement cost (\$); d is the real

discount rate, with a value of 6% in this paper; n is the project lifetime, in years; d' is the original discount rate, with a value of 6% in this paper; f is the inflation rate, with a value of 0% in this paper.

LCOE represents the average cost per unit of energy generated within a particular system over lifetime of the project ($/kWh). The equations of LCOE can be presented by[53]

$$\mathrm{LCOE} = \frac{C_{\mathrm{A}}}{E_{\mathrm{s}}}, \tag{21}$$

where E_{s} is total electrical load supplied that is equal to the sum of primary load and deferrable load (kWh).

2.3 Sensitivity Analysis

A sensitivity analysis has been conducted to quantify the effect of input variables on the pivotal parameters of the project. Within the simulation platform, the indicators include the LCOE and the NPC. The capital cost of the equipment is a significant factor among the variables. In the sensitivity analysis, the influence of geography is also considered, according to the typical weather data.

3 Results and Discussion

3.1 Performance Comparison of Optimized System, Over designed System and under Designed System

3.1.1 Components Capacity

A time series simulation is conducted to find the lowest LCOE and NPC while satisfying technical and economic constraints. The optimized results include LCOE, NPC, component size, energy output, excess energy, unmet load and shortage capacity, as presented in Table 7. Three configurations PV/WT/PHS (case-1), PV/PHS (case-2) and WT/PHS (case-3) are considered for the analysis. It is evident from Table 7 that the optimized system (case-1) consists of 522 kW PV, 150 kW WT, 253 kW converter and 5 390 kWh PHS capacity. PV/PHS system obtains the second priority in economic performance, which consists of 682 kW PV, 255 kW converter and 6 125 kWh PHS. WT/PHS configuration includes 1 720 kW WT, 489 kW converter, and 10 780 kWh PHS.

Table 7 Optimization results of configurations

Characteristics	Unit	PV/WT/PHS	PV/PHS	WT/PHS
		case-1	case-2	case-3
PV capacity	kW	522	682	0
WT capacity	kW	150	0	1 720
PHS capacity	kWh	5 390	6 125	10 780
Battery capacity	kWh	0	0	0
Converter capacity	kW	253	255	489

3.1.2 Economic Performance

The costs of components are described in Fig 7. PV/WT/PHS system obtains the priority in economic performance with its LCOE of 0.139 $/kWh. In case-1, the NPC of the system is $1.17M and total capital cost is $1.07M. Among the various components, PHS system represents the largest cost share, accounting for 45.3% of the total capital cost. This is followed by the PV system (35.0%), the WT (12.6%), and the converter (7.1%). In case-2, the LCOE for PV/PHS is 0.144 $/kWh and the NPC is $1.22M, which shows that case-2 can rival the optimal configuration (case-1). PHS consumes nearly 49.4% of initial capital cost and PV takes 43.8%. WT/PHS (case-3) is the most expensive option among the three configurations comprising PHS with the expense of WT ($1.55M) and PHS ($0.97M), which exhibits a relatively higher LCOE of 0.352 $/kWh and NPC of $2.98M due to the expense of WT ($1.55M) and PHS ($0.97M).

The analysis demonstrates that among the proposed system configurations, the PV/Wind/PHS-based system achieves the lowest LCOE at 0.139 $/kWh. Notably, the optimal system necessitates a smaller capacity of PHS compared to case-2 and case-3 to meet the demand. While other configurations may fulfill the load demand with varying equipment sizes and costs, the PV/WT/PHS system emerges as the optimal choice. In the context of system optimization, it is economically beneficial to satisfy a portion of the peak load demand, rather than the entire supply, when the peak demand at any given time step is exceptionally high. In such scenarios, a small amount of unmet load may occur. However, if peak load can be fully met, the

system inherently necessitates the inclusion of high-cost equipment that often operates below its full capacity. As a result, the system requires a greater upfront capital investment, leading to a subsequent elevation in LCOE.

3.1.3 Techno Performance

The energy output, excess energy and unmet load are shown in Fig 8. In case-1, PV contributes 921 MWh/year, nearly 84.4% of total energy generation and WT generates 170 MWh/year (15.6%). The excess energy is 243 MWh/year (22.3%), which is relatively high. The unmet load demand is 1 072 kWh/year, which is insignificant (0.14%) compared to the total load of 738 MWh/year. In case-2, PV can generate 1 202 MWh/year with 332 MWh (27.7%) excess, while the unmet load is only 1 214 kWh/year (0.14%). The excess energy in case-2 is higher than the case-1 configuration since the entire energy supply relies on PV. In case-3, WT can support 1 950 MWh/year, while producing excess energy of 1 112 MWh/year and the excess energy percentage is 57.0%. In case-3 configuration, there exists a large amount of excess energy that cannot be utilized due to the severe imbalance between the source and load. Higher capacity WT and PHS are required to meet energy demand.

The proposed system's technical feasibility is evident from the minimal unmet electric load and negligible capacity shortage across all configurations. The PV/WT/PHS-based system is cost-effective with lower cost and capacity shortages compared to the other two alternative configurations (Fig 8). The analysis reveals that WT contributes significantly less (15.6%) to the total energy generation compared to PV (84.4%). Only 67.6% of the electricity generated is utilized to satisfy annual demands, while 22.3% remains excess due to transmission and conversion inefficiencies. The integration of PV, WT, and PHS can contribute to meeting peak load demands, which is economically and environmentally competitive when compared to other hybrid system studies.

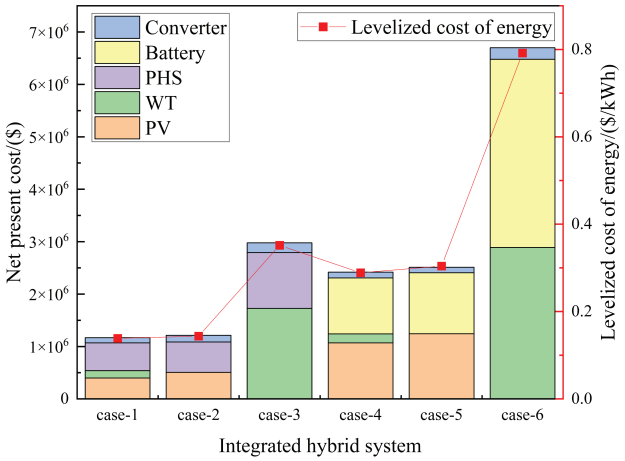

Fig 7 NPC and LCOE of different systems

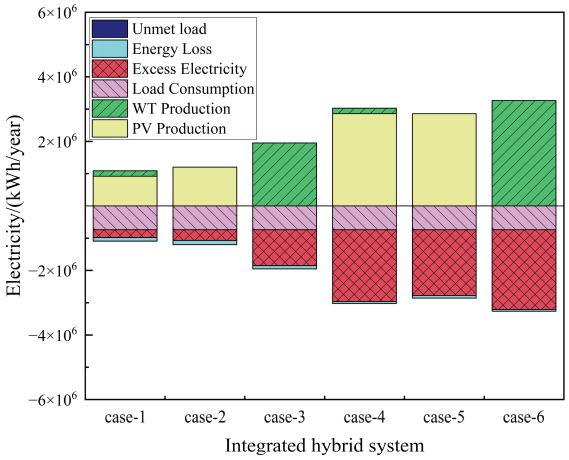

Fig 8 Electricity production and expenditure

3.2 Comparison with Lithium-ion Battery Storage System

Conventional storage components would be compared to determine the optimal storage unit for a hybrid system. This study attempts to compare PHS with battery storage considering ganalogous hybrid configurations. Observations have revealed that the PHS is advantageous over battery-based systems, both in technical and economic terms. The comparison is presented and discussed concisely. The study encompasses three distinct configurations: PV/Wind/Battery (case-4), PV/Battery (case-5), and Wind/Battery (case-6), to facilitate comprehensive comparisons.

The optimized results for hybrid configurations are summarized in Table 8. The PV/WT/Battery system of case-4 has the lowest LCOE and NPC of 0.289 $/kWh and $2.445M, respectively followed by PV/Battery of case-5 (LCOE of 0.304 $/kWh, NPC of $2.576M) and WT/Battery of case-6 (LCOE 0.792 $/kWh, NPC $6.700M). The optimal system (case-4) comprises 1 620 kW PV, 150 kW WT, 269 kW converter and 2 000 kWh Li battery. PV can generate the maximum electricity (2 856 MWh/year), whereas WT delivers 170 MWh/year in total. The excess energy amounts to 2 223 MWh/year (73.5%). On the other hand, the case-5 configuration comprises 1 620 kW PV panels and 2 600 kWh battery. The system produces 2 856 MWh/year. While the excess electricity is 2 039 MWh/year (71.4%) in case-5 with the unmet load of 777 kWh/year (0.11%). WT/Battery system comprises 2 880 kW WT, which generates electricity of 3 265 MWh/year. In case-6, excess electricity is 2 470 MWh (75.7%), and the unmet load is 1 204 kWh/year (0.16%).

If the energy storage system is switched from PHS to batteries, the LCOE will more than double the original cost. The results indicate that battery storage is significantly more costly than PHS, which tends to result in a smaller deployed storage capacity and a relatively higher investment in generation capacity to ensure system reliability. The shortage of energy storage cannot make full use of the large amount of power generated by WT generators. The excess energy will be dumped in off-grid scenarios, which may lead to the waste of energy and increase in cost.

3.3 Comparison with Diesel-Only System

The proposed renewable energy-based system without diesel generators can operate with zero emissions. Comparative analysis is conducted with a system based on the diesel generator to assess its economic and environmental viability. This study evaluates the hybrid system against diesel generators in terms of LCOE, NPC and emissions. The detailed cost components and optimized results are outlined in Table 9. Specifically, the LCOE and NPC of the DG-only system stand at 0.57 \$/kWh and \$4.84M, respectively.

In DG-only system, 251 277 liters of diesel fuel would be consumed to generate 839 MWh electricity with 657 746 kg of CO_2 emission annually. In addition, other emissions data are listed in Table 10. The amounts of carbon monoxide, sulfur dioxide and nitrogen oxides are 4 146 kg/year, 1 611 kg/year and 3 895 kg/year. The proposed PV/WT/PHS hybrid system emerges as a financially and environmentally favorable alternative to DG-only system, according to the analysis.

Table 8 System configuration with battery storage

Characteristics	Unit	PV/WT/Battery	PV/Battery	WT/Battery
		case-4	case-5	case-6
PV capacity	kW	1 620	1 620	0
WT capacity	kW	150	0	2 880
Battery capacity	kWh	2 000	2 600	7 400
Converter capacity	kW	269	244	577
Electricity production	MWh/year	3 026	2 856	3 265
Load consumption	MWh/year	738	738	738
Excess electricity	MWh/year	2 223	2 039	2 470
Unmet load	kWh/year	1 139	777	1 204
PV production	MWh/year	2 856	2 856	0
WT production	MWh/year	170	0	3 265
NPC	\$	2.445×10^6	2.576×10^6	6.700×10^6
LCOE	\$/kWh	0.289	0.304	0.792
Operating cost	\$/year	40 930	49 083	149 535
Initial capital	\$	1.98×10^6	2.01×10^6	4.99×10^6
PV capital cost	\$	1.16×10^6	1.16×10^6	0.00
WT capital cost	\$	1.40×10^5	0.00	2.59×10^6
Converter capital cost	\$	8.00×10^4	7.00×10^4	1.70×10^5
Battery capital cost	\$	6.00×10^5	7.80×10^5	2.22×10^6

Table 9 Results based on DG system

Characteristics	Unit	PV/WT/DG/PHS	PV/WT/PHS	DG/PHS	DG-only
PV capacity	kW	611	522	0	0
WT capacity	kW	90	150	0	0
DG capacity	kW	270	0	270	270
PHS capacity	kWh	3 185	5 390	1 470	0
Converter capacity	kW	212	253	147	0
Electricity production	MWh/year	1 206	1 091	860	839
Load consumption	MWh/year	739	738	739	739
Excess electricity	MWh/year	350	243	0	100
Unmet load	kWh/year	54.4	1 065	0	0
NPC	\$	1.12×10^6	1.17×10^6	3.65×10^6	4.84×10^6
LCOE	\$/kWh	0.13	0.14	0.43	0.57

Table 10 Emissions of DG-only system

Parameter	Unit	Value
Carbon dioxide	kg/year	657 746
Carbon monoxide	kg/year	4 146
Unburned hydrocarbons	kg/year	181
Particulate matter	kg/year	25
Sulfur dioxide	kg/year	1 611
Nitrogen oxides	kg/year	3 895

3.4 The Performance of Different Photovoltaic Tracking Methods

Systems with optional tracking methods are simulated to analyze the impact of photovoltaic tracking methods. Fig 9 shows the economic indicators of hybrid energy systems configured with different PV tracking systems and adjustment strategies. The types of PV include fixed, horizontal monthly-adjustment (HM), horizontal weekly-adjustment (HW), horizontal daily-adjustment (HD), horizontal continuous-adjustment (HC), vertical adjustment (VC) and dual-axis (DA).

The analysis reveals that the fixed PV system incurred a higher NPC averaging $1.17M while the dual-axis system can achieve a lower NPC (about $1.14M). Similarly, the fixed PV system has a higher LCOE of approximately 0.139 $/kWh while the dual-axis system has the lowest LCOE of 0.135 $/kWh. In addition, the time interval of adjustment can affect the performance of PV, and the continuous strategy is the most competitive type in horizontal axis. However, the performance gap among the last three approaches is not prominent.

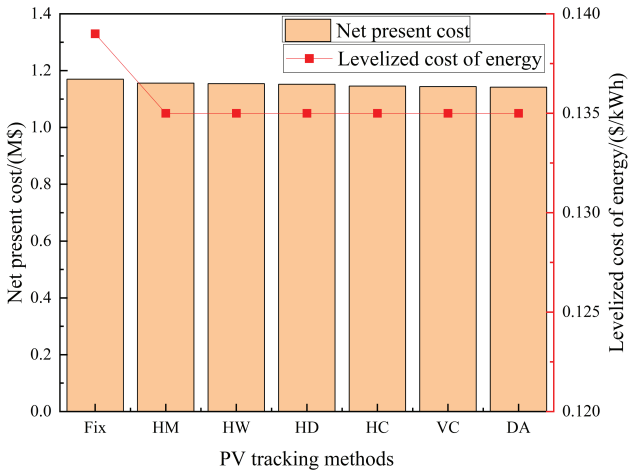

Fig 9 NPC and LCOE of different PV tracking methods

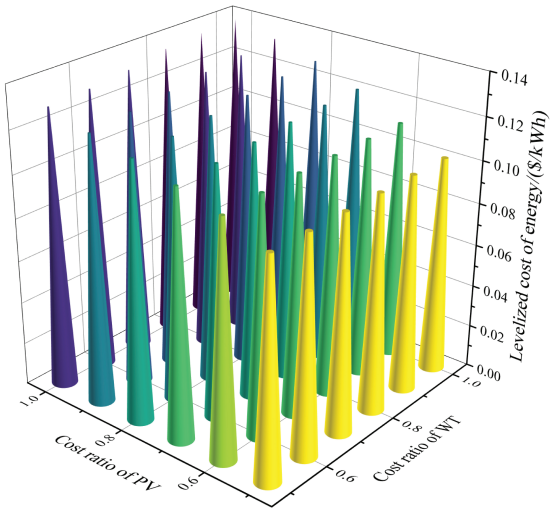

Fig 10 LCOE of different cost ratios of PV and WT

3.5 Sensitivity Analysis of PV/WT/PHS System

3.5.1 The Effects of Capital Cost

Sensitivity analysis is conducted under the adjustment of cost of PV and WT. The cost ratio is the ratio of the proposed cost to the actual cost. As shown in Fig 10, the value of cost ratio varies from 1.0 to 0.5 with a 0.1 step interval. The results show that the reduction of the component's cost can significantly reduce the NPC and LCOE of the PV/WT/PHS system. The system with the current price can obtain an LCOE of 0.119 $/kWh, while the lowest LCOE can be 0.092 7 $/kWh when the cost ratios of PV and WT are both set as 0.6 ideally. It can be noted that the power generation components matter to the capacity design and investment of energy systems. In this case, the impact of PV cost on the change in LCOE may be greater than that of WT price because the capacity of PV accounts for a larger proportion of the total cost.

Though the cost reduction can achieve a better economic performance, it may cause more energy excess consequently. As shown in Fig 11, the percentage of excess energy may rise when the capital cost of PV decreases. This is because the reduction in module costs allows for the design of larger-scale generation modules within the proposed budget amount. However, the load of the user at each time is limited and cannot fully absorb the power generation. The results mean that the system may be over designed to fulfill the loads of some extreme cases, and the scaled-up capacity can lead to more resources not being used efficiently. However, when the cost of WT decreases, the percentage of excess energy may consequently fall as well.

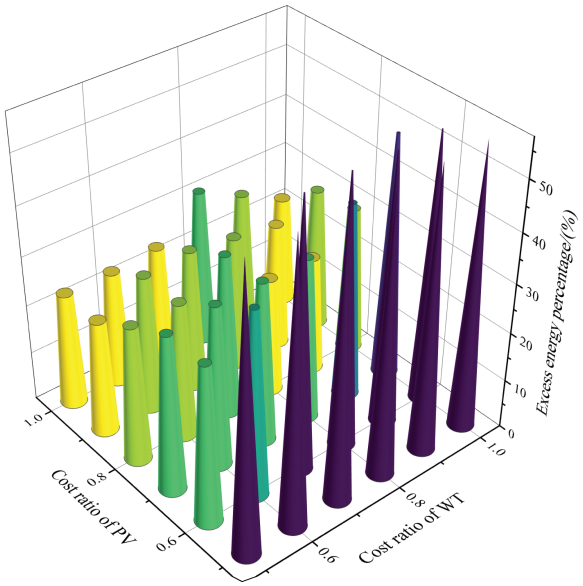

Fig 11 Excess energy percentage of different cost ratios of PV and WT

3.5.2 The Performance in Different Regions of Xinjiang

To investigate the potential of renewable energy resources in Northwest China, several regions are chosen for the design of hybrid energy systems. The performance of PV/WT/PHS (case-1), PV/PHS (case-2) and WT/PHS (case-3) were analyzed. The results in Table 11 reveal that PV/WT/PHS and PV/PHS systems can be competitive at a certain expense. The optimal PV/WT/PHS system is in Kashgar, with an LCOE of 0.119 $/kWh. Moreover, Kashgar also has the lowest LCOE of PV/PHS, which is 0.117 $/kWh. The results mean that Kashgar has a more balanced renewable energy resource to generate electricity because of its meteorological condition. And the highest LCOE of the case-1 configuration is 0.148 $/kWh in Altay, while the highest LCOE of the case-3 configuration is 0.158 $/kWh in Tacheng. The results show that the WT/PHS systems are more expensive than PV/WT/PHS and PV/PHS. The best WT/PHS (case-3) configuration can obtain the lowest LCOE of 0.213 $/kWh in Karamay, with a balanced resource of wind and solar irradiation conditions for renewable energy. While the most expensive WT/PHS system may get an LCOE of 1.200 $/kWh in Bortala because of the shortage of wind resources. According to the local climatic conditions, solar energy has an economic advantage over wind energy. Therefore, investors should choose to expand the scale of the PV system as much as possible. If funds are still available, the construction of WT can increase the diversity of energy sources. However, it is still not advisable to entirely choose wind power as a single source of energy according to the economic indicators.

Table 11 LCOE of systems in different regions ($/kWh)

Region	HPBS	PV/PHS	WT/PHS
Urumqi	0.135	0.139	0.323
Karamay	0.132	0.149	0.213
Turpan	0.142	0.141	0.813
Hami	0.129	0.128	0.812
Changji	0.143	0.142	1.027
Bortala	0.145	0.144	1.200
Bayingolin	0.138	0.138	0.817
Aksu	0.134	0.134	1.187
Kizilsu	0.119	0.117	0.907
Kashgar	0.119	0.117	0.907
Hotan	0.132	0.134	0.443
Ili	0.138	0.138	0.481
Tacheng	0.131	0.158	0.315
Altay	0.148	0.147	0.444
Shihezi	0.135	0.139	0.323
Aral	0.140	0.142	0.512
Tumshuk	0.127	0.126	0.658
Wujiaqu	0.135	0.139	0.323
Beitun	0.148	0.147	0.444
Tiemenguan	0.138	0.138	0.817
Shuanghe	0.145	0.144	1.190
Kokdala	0.138	0.138	0.481
Kunyu	0.119	0.117	0.907
Huyanghe	0.132	0.149	0.213

4 Conclusions

This paper presents an analysis of the potential for a renewable energy-based power supply system in Xinjiang, focusing on the cost of energy (LCOE) and net present cost (NPC) of systems comprising photovoltaic (PV) and wind turbines (WT) with pumped hydro storage (PHS) and battery bank. The PV/WT/PHS option is the optimal configuration with the LCOE of 0.139 $/kWh which is lower than the LCOE of PV/PHS (0.144 $/kWh) and WT/PHS (0.352 $/kWh). Diverse resources can provide valuable contributions to the power supply and solar power is cheaper under local weather conditions.

If the energy storage system is switched from PHS to batteries, the LCOE will be more than 200% of the PHS cost. Compared to a diesel-only system, the renewable energy system can reduce 657 746 kg of CO_2 emission annually and obtain lower LCOE because of the renewable resources. In addition, the PV tracking system can promote PV generation. The dual-axis system has the lowest LCOE of 0.135 $/kWh. As the price of the module decreases, the LCOE will decrease while the excess energy percentage may increase. The optimal PV/WT/PHS system is in Kashgar, with an LCOE of 0.119 $/kWh. In most regions of Xinjiang, renewable energy systems dominated by PV have economic advantages over those dominated by WT.

Overall, the study demonstrates the potential for a renewable energy-based power supply system to supply electricity to a remote community at a lower cost and reduce greenhouse gas emissions. However, the results also show that excess energy matters to techno-economic performance. Therefore, it is important to consider trade-offs when designing a power supply system for remote areas.

References:

[1] STERN P C, SOVACOOL B K, DIETZ T. Towards a science of climate and energy choices[J]. Nature Climate Change, 2016, 6(6): 547-555.

[2] ZHANG Z, ZHAO Y L, CAI H Y, et al. Influence of renewable energy infrastructure, Chinese outward FDI, and technical efficiency on ecological sustainability in belt and road node economies[J]. Renewable Energy, 2023, 205: 608-616.

[3] TONG D, ZHANG Q, ZHENG Y X, et al. Committed emissions from existing energy infrastructure jeopardize 1.5 ℃ climate target[J]. Nature, 2019, 572(7769): 373-377.

[4] WU S. A systematic review of climate policies in China: Evolution, effectiveness, and challenges[J]. Environmental Impact Assessment Review, 2023, 99: 107030.
[5] SUN G B, LI G Z, DILANCHIEV A, et al. Promotion of green financing: Role of renewable energy and energy transition in China[J]. Renewable Energy, 2023, 210: 769-775.
[6] HESTY N W, FAUZIAH K, AMINUDDIN, et al. A comprehensive analysis of wind power integrated with solar and hydrogen storage systems: Case study of Java's Southern coast[J]. International Journal of Hydrogen Energy, 2024, 10: 1-14.
[7] WANG X X, XIAO X M, ZHANG X, et al. Characterization and mapping of photovoltaic solar power plants by Landsat imagery and random forest: A case study in Gansu Province, China[J]. Journal of Cleaner Production, 2023, 417: 138015.
[8] WANG Y H, QIN Y Y, WANG K, et al. Where is the most feasible, economical, and green wind energy? Evidence from high-resolution potential mapping in China[J]. Journal of Cleaner Production, 2022, 376: 134287.
[9] ZHOU Y K. Renewable-storage sizing approaches for centralized and distributed renewable energy: A state-of-the-art review[J]. Journal of Energy Storage, 2024, 100: 113688.
[10] GENSLER A, SICK B, VOGT S. A review of uncertainty representations and metaverification of uncertainty assessment techniques for renewable energies[J]. Renewable and Sustainable Energy Reviews, 2018, 96: 352-379.
[11] ZAKARIA A, ISMAIL F B, HOSSAIN LIPU M S, et al. Uncertainty models for stochastic optimization in renewable energy applications[J]. Renewable Energy, 2020, 145: 1543-1571.
[12] ZHANG Y J, MA T, YANG H X. A review on capacity sizing and operation strategy of grid-connected photovoltaic battery systems[J]. Energy and Built Environment, 2024, 5(4): 500-516.
[13] WANG W, YUAN B Q, SUN Q, et al. Application of energy storage in integrated energy systems: A solution to fluctuation and uncertainty of renewable energy[J]. Journal of Energy Storage, 2022, 52: 104812.
[14] LIU Y X, HE Q, SHI X P, et al. Energy storage in China: Development progress and business model[J]. Journal of Energy Storage, 2023, 72: 108240.
[15] BASNET S, DESCHINKEL K, LE MOYNE L, et al. A review on recent standalone and grid integrated hybrid renewable energy systems: System optimization and energy management strategies[J]. Renewable Energy Focus, 2023, 46: 103-125.
[16] ZHANG O, YU S K, LIU P K. Development mode for renewable energy power in China: Electricity pool and distributed generation units[J]. Renewable and Sustainable Energy Reviews, 2015, 44: 657-668.
[17] XIA H, DAI L, SUN L P, et al. Analysis of the spatiotemporal distribution pattern and driving factors of renewable energy power generation in China[J]. Economic Analysis and Policy, 2023, 80: 414-428.
[18] LI X, ZHU C K, LIU Y Z. Traction power supply system of China high-speed railway under low-carbon target: Form evolution and operation control[J]. Electric Power Systems Research, 2023, 223: 109682.
[19] KUMAR K P, SARAVANAN B. Recent techniques to model uncertainties in power generation from renewable energy sources and loads in microgrids: A review[J]. Renewable and Sustainable Energy Reviews, 2017, 71: 348-358.
[20] VAZIRI RAD M A, KASAEIAN A, NIU X F, et al. Excess electricity problem in off-grid hybrid renewable energy systems: A comprehensive review from challenges to prevalent solutions[J]. Renewable Energy, 2023, 212: 538-560.
[21] COME ZEBRA E I, VAN DER WINDT H J, NHUMAIO G, et al. A review of hybrid renewable energy systems in mini-grids for off-grid electrification in developing countries[J]. Renewable and Sustainable Energy Reviews, 2021, 144: 111036.
[22] ORTEGA-ARRIAGA P, BABACAN O, NELSON J, et al. Grid versus off-grid electricity access options: A review on the economic and environmental impacts[J]. Renewable and Sustainable Energy Reviews, 2021, 143: 110864.
[23] THIRUNAVUKKARASU M, SAWLE Y, LALA H. A comprehensive review on optimization of hybrid renewable energy systems using various optimization techniques[J]. Renewable and Sustainable Energy Reviews, 2023, 176: 113192.
[24] BANESHI M, HADIANFARD F. Techno-economic feasibility of hybrid diesel/PV/wind/battery electricity generation systems for non-residential large electricity consumers under southern Iran climate conditions[J]. Energy Conversion and Management, 2016, 127: 233-244.
[25] ABDELHADY S. Techno-economic study and the optimal hybrid renewable energy system design for a hotel building with net zero energy and net zero carbon emissions[J]. Energy Conversion and Management, 2023, 289: 117195.
[26] CHISALE S W, ELIYA S, TAULO J. Optimization and design of hybrid power system using HOMER Pro and integrated CRITIC-PROMETHEE II approaches[J]. Green Technologies and Sustainability, 2023, 1(1): 100005.
[27] KHALIL L, LIAQUAT BHATTI K, ARSLAN IQBAL AWAN M, et al. Optimization and designing of hybrid power system using HOMER Pro[J]. Materials Today: Proceedings, 2021, 47: S110-S115.
[28] HOSSAIN M, MEKHILEF S, OLATOMIWA L. Performance evaluation of a stand-alone PV-wind-diesel-battery hybrid system feasible for a large resort center in South China Sea, Malaysia[J]. Sustainable Cities and Society, 2017, 28: 358-366.
[29] KHAN M J, YADAV A K, MATHEW L. Techno economic feasibility analysis of different combinations of PV-wind-diesel-battery hybrid system for telecommunication applications in different cities of Punjab, India[J]. Renewable and Sustainable Energy Reviews, 2017, 76: 577-607.
[30] FODHIL F, HAMIDAT A, NADJEMI O. Potential, optimization and sensitivity analysis of photovoltaic-diesel-battery hybrid energy system for rural electrification in Algeria[J]. Energy, 2019, 169: 613-624.
[31] GOMAA M R, AL-BAWWAT A K, AL-DHAIFALLAH M, et al. Optimal design and economic analysis of a hybrid renewable energy system for powering and desalinating seawater[J]. Energy Reports, 2023, 9: 2473-2493.
[32] DAS B K, ZAMAN F. Performance analysis of a PV/diesel hybrid system for a remote area in Bangladesh: Effects of dispatch strategies, batteries, and generator selection[J]. Energy, 2019, 169: 263-276.
[33] THIRUNAVUKKARASU M, SAWLE Y. Design, analysis and optimal sizing of standalone PV/diesel/battery hybrid energy system using HOMER[J]. IOP Conference Series: Materials Science and Engineering, 2020, 937(1): 012034.

[34] SWARNKAR N M, GIDWANI L. Analysis of hybrid energy system for supply residential electrical load by HOMER and RETScreen: A case in Rajasthan, India[C]//2016 International Conference on Recent Advances and Innovations in Engineering (ICRAIE). Jaipur, India. IEEE, 2016: 1-6.
[35] MIAO H Y, YU Y D, KHARRAZI A, et al. Multi-criteria decision analysis for the planning of island microgrid system: A case study of Yongxing island, China[J]. Energy, 2023, 284: 129264.
[36] ABDIN Z, MÉRIDA W. Hybrid energy systems for off-grid power supply and hydrogen production based on renewable energy: A techno-economic analysis[J]. Energy Conversion and Management, 2019, 196: 1068-1079.
[37] CHAURASIA R, GAIROLA S, PAL Y. Technical, economic, and environmental performance comparison analysis of a hybrid renewable energy system based on power dispatch strategies[J]. Sustainable Energy Technologies and Assessments, 2022, 53: 102787.
[38] ISLAM M S, DAS B K, DAS P, et al. Techno-economic optimization of a zero emission energy system for a coastal community in Newfoundland, Canada[J]. Energy, 2021, 220: 119709.
[39] LI C, ZHOU D Q, WANG H, et al. Techno-economic performance study of stand-alone wind/diesel/battery hybrid system with different battery technologies in the cold region of China[J]. Energy, 2020, 192: 116702.
[40] FOSSO TAJOUO G, TIAM KAPEN P, DJANNA KOFFI F L. Techno-economic investigation of an environmentally friendly small-scale solar tracker-based PV/wind/battery hybrid system for off-grid rural electrification in the mount bamboutos, Cameroon[J]. Energy Strategy Reviews, 2023, 48: 101107.
[41] BAHRAMARA S, MOGHADDAM M P, HAGHIFAM M R. Optimal planning of hybrid renewable energy systems using HOMER: A review[J]. Renewable and Sustainable Energy Reviews, 2016, 62: 609-620.
[42] YANG J, LI G Q, GAN Y X, et al. Role of the tropical Indian Ocean in orbitally induced mid-Holocene precipitation variation in Northwest China[J]. Quaternary Science Reviews, 2023, 317: 108285.
[43] WU Y J, MU H L, WU S Y, et al. Changes in mean and extreme homogeneous precipitation in China during 1960—2020[J]. Atmospheric Research, 2023, 292: 106891.
[44] WEN X H, WU X Q, GAO M. Spatiotemporal variability of temperature and precipitation in Gansu Province (Northwest China) during 1951—2015[J]. Atmospheric Research, 2017, 197: 132-149.
[45] ZHANG T P, STACKHOUSE P W, MACPHERSON B, et al. A CERES-based dataset of hourly DNI, DHI and global tilted irradiance (GTI) on equatorward tilted surfaces: Derivation and comparison with the ground-based BSRN data[J]. Solar Energy, 2024, 274: 112538.
[46] MANDAL S, DAS B K, HOQUE N. Optimum sizing of a stand-alone hybrid energy system for rural electrification in Bangladesh[J]. Journal of Cleaner Production, 2018, 200: 12-27.
[47] International Renewable Energy Agency. Renewable power generation costs in 2020[EB/OL]. (2021-06-22)[2024-10-26]. https://www.irena.org/-/media/Files/IRENA/Agency /Publication/2021/Jun/IRENA_Power_Generation_Costs_2020.pdf.
[48] DASH R L, MOHANTY B, HOTA P K. Energy, economic and environmental (3E) evaluation of a hybrid wind/biodiesel generator/tidal energy system using different energy storage devices for sustainable power supply to an Indian archipelago[J]. Renewable Energy Focus, 2023, 44: 357-372.
[49] AMINI M, NAZARI M H, HOSSEINIAN S H. Optimal energy management of battery with high wind energy penetration: A comprehensive linear battery degradation cost model[J]. Sustainable Cities and Society, 2023, 93: 104492.
[50] ZHANG Y J, MA T, ELIA CAMPANA P, et al. A techno-economic sizing method for grid-connected household photovoltaic battery systems[J]. Applied Energy, 2020, 269: 115106.
[51] JAVED M S, MA T, JURASZ J, et al. A hybrid method for scenario-based techno-economic-environmental analysis of off-grid renewable energy systems[J]. Renewable and Sustainable Energy Reviews, 2021, 139: 110725.
[52] XU X G, ZHANG Z, YUAN J W, et al. Design and multi-objective comprehensive evaluation analysis of PV-WT-BG-battery hybrid renewable energy systems in urban communities[J]. Energy Conversion and Management, 2023, 18: 100357.
[53] MA W W, FAN J Q, FANG S, et al. Techno-economic potential evaluation of small-scale grid-connected renewable power systems in China[J]. Energy Conversion and Management, 2019, 196: 430-442.

责任编辑：刘 敏